Influence of Aerodynamic Model Assumptions on the Wind-Vehicle-Bridge Interaction

Igor Kavrakov, Guido Morgenthal

Bauhaus University, Weimar, Germany

Alfredo Camara

City University, London, UK

Contact: igor.kavrakov@uni-weimar.de

Abstract

Wind-induced vibrations are commonly the leading action in the ultimate and serviceability state of the long-span bridges. There is a multitude of aerodynamic models for simulating wind action on a bridge deck based on various theories. Within this study, the influence of the implied assumptions in the aerodynamic models is studied regarding the Wind-Vehicle-Bridge Interaction (WVBI). As a reference object, a suspension bridge under gusty wind is chosen, for which the aerodynamic models are evaluated based on accident and comfort criteria. Different aspects of the WVBI are also included such as road roughness and wind forces on the vehicle.

Keywords: Wind-Vehicle-Bridge Interaction, Long-Span Bridges, Wind-Induced Vibrations

1 Introduction

Flexible long span suspension bridges are prone to wind-induced vibrations. The light weight, low structural damping and aerodynamic shape make this type of structures a true challenge for a structural engineer to determine their response. In the ultimate limit state, high wind speeds are governing for determining section forces and displacements along with checks against instability such as flutter. For the serviceability limit state, the situation is quite different, since prescribed deformation, driving stability and comfort criteria are governing. Usually, these criteria need to be fulfilled for lower wind speeds and depend on the bridge type and its design purpose. Some typical criteria include: limiting the acceleration perceived by drivers and pedestrians, derailment of trains and accident speeds for vehicles. In this paper, the accident and comfort criteria based on acceleration in the cabin and loss of contact for road-wheel for light road trucks are studied passing a suspension bridge excited by turbulent wind. In WVBI, modeling the wind forces can be twofold, namely: the wind forces acting on the vehicle and on the bridge. The first type is commonly done by the quasi-static formulation using predefined static wind coefficients in case of WVBI, while there are many aerodynamic models for the wind forces acting on the bridge. The aerodynamic models for forces acting on the bridge deck due to its motion (self-excited) and incoming turbulence (buffeting) are developed mainly on two theories: the quasi steady and the linear unsteady theory. The first types of models typically include the nonlinear relation between the static wind coefficients and angle of attack, neglecting the rise time of the self-excited and buffeting forces described by the fluid memory and aerodynamic admittance respectively. For streamed lined decks, the coupling between the vertical and torsional motion becomes a crucial phenomenon leading to coupled flutter occurring at high wind velocities. The motivation comes from the question whether is always necessary to use the most complex aerodynamic models, which come at the price of a higher number of input parameters, numerical uncertainty and computational time. If this is not the case, then perhaps using simpler aerodynamic models would yield in satisfactory results for the WVBI. The goal of this study is to identify which of these assumptions implied in the aerodynamic models have a significant influence on the comfort and accident criteria for light trucks.

2 Wind-Vehicle-Bridge Interaction

The WVBI presents a coupled problem between the vehicle and the bridge through contact forces with an additional forcing component due to the wind action. During the motion of the vehicle, the contact points change with time, inducing a dynamic action on the bridge. Assuming no loss of contact and ignoring the driver's behavior, the discrete formulation utilizing modal coordinates $\boldsymbol{q_b}$ for the bridge and displacement vector $\boldsymbol{q_v}$ with their time derivatives can be formulated as:

$$\begin{bmatrix} M_b & \\ & M_v \end{bmatrix}\begin{Bmatrix} \ddot{\boldsymbol{q}}_{\boldsymbol{b}} \\ \ddot{\boldsymbol{q}}_{\boldsymbol{v}} \end{Bmatrix} + \begin{bmatrix} C_b + C_b^v & C_{b,v} \\ C_{v,b} & C_v \end{bmatrix}\begin{Bmatrix} \dot{\mathbf{q}}_{\mathbf{b}} \\ \dot{\mathbf{q}}_{\mathbf{v}} \end{Bmatrix} + \begin{bmatrix} K + K_b^v & K_{b,v} \\ K_{v,b} & K_v \end{bmatrix}\begin{Bmatrix} \boldsymbol{q_b} \\ \boldsymbol{q_v} \end{Bmatrix} = \begin{Bmatrix} \Phi^T\left(\mathbf{f_{b,w}} + \mathbf{f_{b,r}}\right) \\ \boldsymbol{f}_{\boldsymbol{v},\boldsymbol{g}} + \boldsymbol{f}_{\boldsymbol{v},\boldsymbol{r}} + \boldsymbol{f}_{\boldsymbol{v},\boldsymbol{w}} \end{Bmatrix}, \tag{1}$$

where the M_b, C_b, K_b present the modal mass, damping and stiffness matrices of the bridge respectively, and M_v, C_v, K_v are the mass, damping and stiffness matrices of the vehicle. These matrices are constant through the motion of the vehicle. The damping and stiffness coupling terms $C_{v,b} = C_{v,b}, K_{v,b} = K_{v,b}$ and the terms describing the contribution of the vehicle to the damping and stiffness matrices of the bridge K_b^v, $K_{b,v}$ are dependent on the vehicle position and thus, are time variant. Hahn [1] offers an extensive formulation of these matrices, which are used in this study as well. The variations of the ideal road surface are accounted for by the roughness forcing vector acting on the vehicle and bridge through the forcing vectors $\boldsymbol{f_{v,r}}$ and $\boldsymbol{f_{b,r}}$ as will be shown in the further sections. $\boldsymbol{f_{v,g}}$, $\boldsymbol{f_{v,r}}$ present the gravity and wind force acting on the vehicle, while Φ is a matrix containing the mode shapes. Particular point of interest in this work is the wind force vector acting on the bridge $\boldsymbol{f_{b,w}}$, which can be described by various models based on various assumptions.

Negative wheel-deck reaction forces is attributed to the loss of contact between both and will be interpreted in this study as an overturning accident, in line with previous research works [2]. A code has been developed for the WVBI framework based on input modal information including simulation of wind-time histories and pavement roughness.

2.1 Bridge aerodynamic forcing models

The Fluid-Structure Interaction (FSI) is a complex phenomenon, which in bridge engineering is commonly replicated by semi-analytical models based on flat-plate theory and aerodynamic coefficients to account for the complex aerodynamic behaviour with multiple flow separation points and coupled aerodynamic damping. These coefficients are obtained from experiments or numerical simulations using Computational Fluid Dynamics (CFD). Figure 1 depicts a cross section of a bridge deck with width B excited by wind forces. For this simplified 3 Degree-of-Freedom (DoF) system the wind force vector $\boldsymbol{f_{b,w}} = [F_D\ F_L\ F_M\ ]^T$ includes the drag, lift and moment component, respectively. The modal displacements $\boldsymbol{q_b} = [p\ h\ \alpha\ ]^T$ are constituted of horizontal and vertical displacements and of rotation.

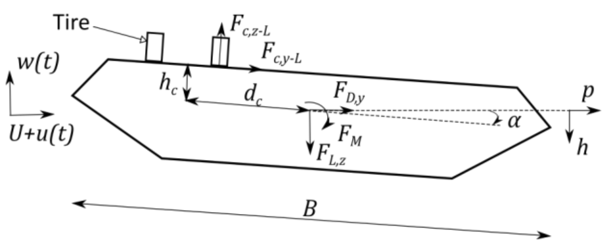

Figure 1. Contact points and aerodynamic forces acting on a bridge deck.

The turbulent wind is typically separated into a horizontal u and a vertical fluctuating component w with a mean wind speed U. There are a large number of semi-analytical models and methods for describing the wind forces. Within this study the Quasi Steady (QS), Linear Quasi Steady (LQS), Linear Unsteady (LU), Modified Quasi Steady (MQS) and the Mode by Mode (MBM) model are considered. A comprehensive study is offered by Wu and Kareem [3]. The QS model takes into account the aerodynamic nonlinearity by the non-linear relationship between the relative angle of attack and the static lift coefficient C_L:

$$F_L = -\tfrac{1}{2}\rho V_{res}^2 B C_L(\alpha_{res}), \tag{2}$$

where ρ is the fluid density. The resultant attack α_{res} constituted by the static α_0, and the instantaneous angle along with the resultant wind velocity V_{res} are defined as :

$$V_{res} = \sqrt{(U + u - \dot{p})^2 + \left(w + \dot{h} + m_{r,i}B\dot{\alpha}\right)^2}, \tag{3}$$

$$\alpha_{res} = \alpha_0 + \alpha + \frac{(w + \dot{h} + m_{r,i}B\dot{\alpha})}{U + u - \dot{p}}. \tag{4}$$

Commonly, the slopes of the static wind coefficients are obtained from wind-tunnel tests, and if the QS model is linearized with respect to the static angle of attack, the LQS model can be obtained. From the above relations, it can be deduced that most of the models include terms dependent on the instantaneous bridge motion, by which they include the effect of aerodynamic damping and stiffness. However, in reality the forces arising from the motion of the structure (self-excited forces) and buffeting forces due to wind fluctuations have a rise time. With this, the forces are dependent not only on the instantaneous bridge displacements, rather than on the whole time history and the oscillation frequencies (ω_i). This unsteady effect is regarded to as the fluid memory effect which is introduced in the LU model by introducing flutter derivatives ($H_i^*(K)$) for the self-excited forces. These are dependent on the reduced frequency of oscillation $H_i^*(K = \frac{U}{\omega B})$ and are introduced in:

$$\begin{aligned} F_{L,z}^{se} = \frac{1}{2}\rho U^2 B \Bigg(& KH_1^*\frac{\dot{h}}{U} + KH_2^*\frac{\dot{\alpha}}{U} + K^2H_3^*\alpha \\ & + K^2H_4^*\frac{h}{U} + KH_5^*\frac{\dot{p}}{U} + K^2H_6^*\frac{p}{B}\Bigg) \end{aligned} \tag{5}$$

For the buffeting forces the rise time is introduced by the aerodynamic admittance function χ:

$$\begin{aligned} F_{L,z}^{b} = -\frac{1}{2}\rho U^2 B \Bigg(& C_L + (C_L' + C_D)\frac{w}{U}\chi_{D,w} \\ & + C_D\frac{2u}{U}\chi_{D,u}\Bigg) \end{aligned} \tag{6}$$

An obvious difficulty in these formulations is that they contain frequency and time dependent terms. One way to introduce them into the time-domain is by employing rational approximation utilizing impulse functions, as it is done in this paper in case of the LU model. The rational approximation in some cases can introduce a degree of numerical uncertainty. If it is assumed that the frequency content at the structural frequencies dominates the motion the flutter derivatives can be interpolated at the structural frequencies. This constitutes the MQS model. However, for high wind velocities and streamlined bridge decks, the vertical and torsional modes couple on the aerodynamic side resulting in a single frequency of oscillation causing divergent amplitudes of oscillation known as coupled flutter instability. In all of the previous models, there was a component in the lift force dependent on the torsional motion. By introducing the MBM model this component is neglected, and in case of the 3-DoF system $H_{2,3,5,6}^* = 0$. The previous defined models contained different kinds of assumptions which are mainly dependent on the shape of the cross section and wind speed. For high turbulence intensities and bluff cross sections, the aerodynamic nonlinearities might a play significant role, while for high reduced velocities and streamlined sections it is unsafe to neglect the aerodynamic coupling. The fluid memory has a higher effect on the response for low reduced velocities; however, the effect of aerodynamic damping is small and thus it might not influence the response. Thus it is intriguing to study the influence of these assumptions on WVBI.

2.2 Vehicle Model

There is a multitude of different vehicles in the literature which can are considered for Vehicle-Bridge Interaction (VBI). Critical types of vehicles in case of wind action are the light trucks due to their light mass and large frontal area. A 12 DoF vehicle model is used in this study which is commonly used in WVBI. It consists of two axles and four wheels simplified as one rigid body with four axle mass blocks and series of springs and viscous dashpots for energy dissipation as depicted on Figure 3. Point contact is assumed between the tires and the deck and the tire elasticity and suspension are modelled with springs. The road surface roughness is simulated as Gaussian random process with zero mean value using the power spectral density function [1]:

$$S(\bar{\varphi}) = A_r\left(\frac{\bar{\varphi}}{\varphi_0}\right)^{-2}, \tag{7}$$

where $\bar{\varphi}$ and φ_0 are the wave number and discontinuity frequency respectively, while and A_r is the road roughness coefficient.

2.3 Vehicle wind forces

The quasi-static approach was utilized for modelling wind forces on vehicle. The wind forces acting on a vehicle (Figure 2) after [2] are:

$$F_i = \frac{1}{2}\rho V_r^2 C_i(\psi)A, \quad F_j = \frac{1}{2}\rho V_r^2 C_j(\psi)Ah_v, \tag{8}$$

where the static coefficients C_i are for drag, side and lift force F_i $(i = D, L, M)$ and C_j are for yawn, rolling and pitching moment F_j $(j = Y, P, R)$ respectivly. The resultant velocity $V_r(V, U, u)$ is a function of the mean wind speed, vehicle speed V and instantaneous horizontal fluctuation u. The resultant angle is depicted on the figure and the values for $C_{i,j}$ are obtained from the cited literature.

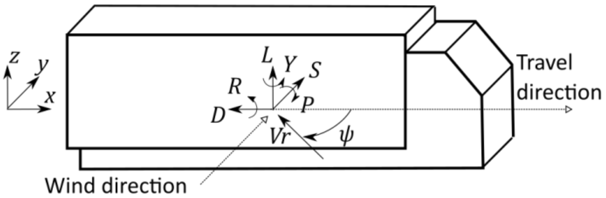

Figure 2.Quasi-static wind forces acting on vehicle.

2.4 Accident and comfort criteria

There have been several definitions of vehicle accident criterion. The most common ones are defined by Colman and Baker [2] for overturning, side-slip and yawning accident. The overturning is defined as a loss of contact on the wheels, while side-slip occurs if the lateral deflection of the vehicle exceeds 0.5m, the yawning accidents occurs if the yawn angle is higher than 0.2 rad. To examine the influence of the aerodynamic models for the wind forces on deck on the vehicle, the negative contact force was set as an accident criterion. A full accident analysis requires either a local vehicle model or a nonlinear iteration for the horizontal contact force. However, most of the studies indicated overturning as a critical criteria. The full accident analysis is beyond the scope of this study. For the driver comfort, different magnitude levels are defined based on ISO 2631 [6] for the Root-Mean-Square (RMS) of weighted resultant acceleration of the driver's seat a_{ds}. The vertical and along wind acceleration time-histories are modified by a frequency weighting factors for the 1/3 octave bands. The RMS is then applied separately on the weighted signals, from which the resultant is obtained.

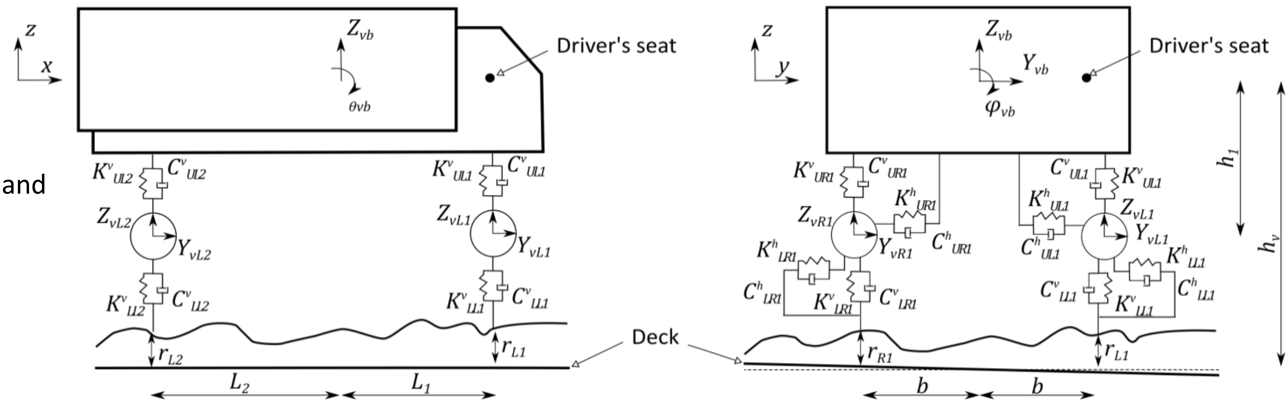

Figure 3. The vehicle model in dynamic analysis: (left) longitudinal section and (right) front view.

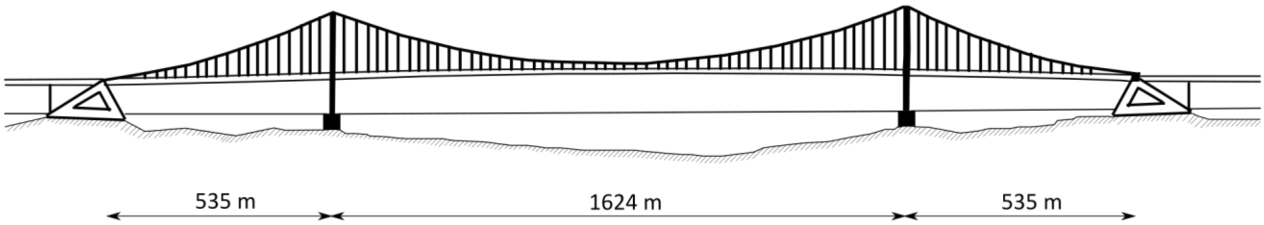

Figure 4. Elevation view of the Great Belt bridge.

3 Application

3.1 Reference object and vehicle parameters

Streamed lined steel box girders are quite often used in long suspension bridges as the light weight and aesthetics are their main assets. The aerodynamic shape reduces the drag forces acting on the bridge; however they are prone to aerodynamic coupling resulting in coupled flutter. In order to emphasize the effects of the implied assumptions in the aerodynamic wind load models, the Great Belt Bridge was chosen as reference object, since it is deeply studied and vast literature exists on its aerodynamic properties. The main span is 1624 m long with two side spans of 535 m each, as depicted in Figure 4. The cross section is 31 m long and its shape is the same as in Figure 1. A Finite Element Model was created and validated against dynamic properties in the existing literature [5]. The first lateral, bending and torsional modes have frequencies of 0.052, 0.1 and 0.278 Hz respectively. The aerodynamic properties were obtained by an in-house CFD code using the Vortex Particle Method (VPM), developed by Morgenthal [6]. The static wind coefficients are depicted on Figure 5, for which good agreement was obtained for the lift and moment coefficients with the wind tunnel results [9]. A typical high sided light truck was used as critical vehicle in windy conditions with wind area A=10.5m^2 and vehicle dimensions L_1=3m, L_2=5m, b=2.2m and h_v=1.5m. The rest of the properties are found in [2] and are omitted here. To simulate traffic on the bridge, a convoy of 20 vehicles were used with 75m distance in between simulating moderate traffic conditions. The path was set on one side of the bridge with horizontal distance of d_c=6.6m to the stiffness centre in order to induce maximum torsional response. The total length of the convoy is 1500m and at certain time instances, all of the vehicles will be on the main span. A road roughness coefficient of 16 m^3/cycle was used, resulting in eight deck-wise correlated profiles, depicted on Figure 6, where separate vertical regions are visible. The analysis was done utilizing the Newmark-beta algorithm for a system in modal coordinates consisting of 22 modes with 0.5% modal damping. Without loss of generality, wind was applied only on deck for 5 different mean wind speeds ranging from 5 to 35 with 6% and 8% vertical and longitudinal turbulence intensity, respectively.

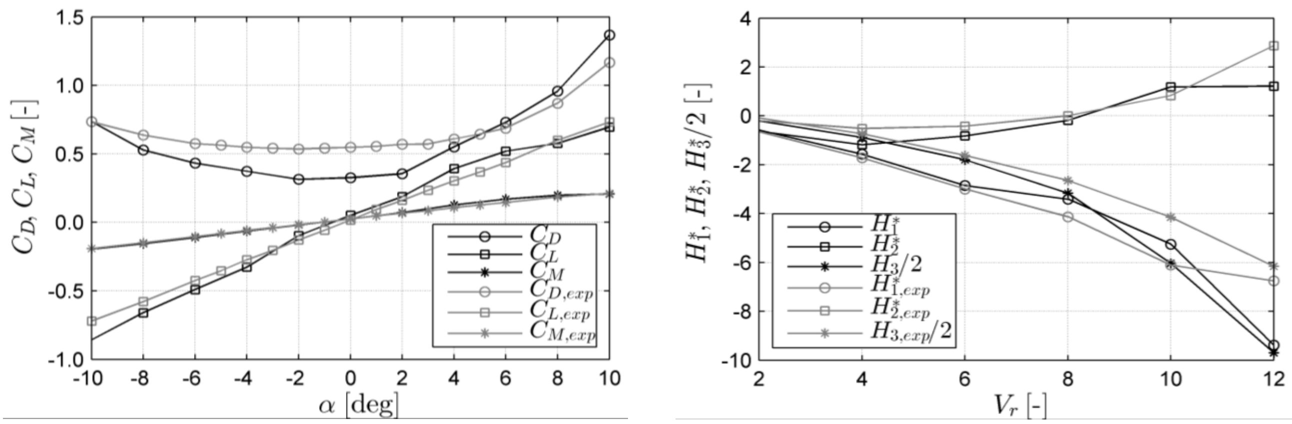

Figure 5. Comparison with experimental data: (left) static wind coefficients; (right) flutter derivatives.

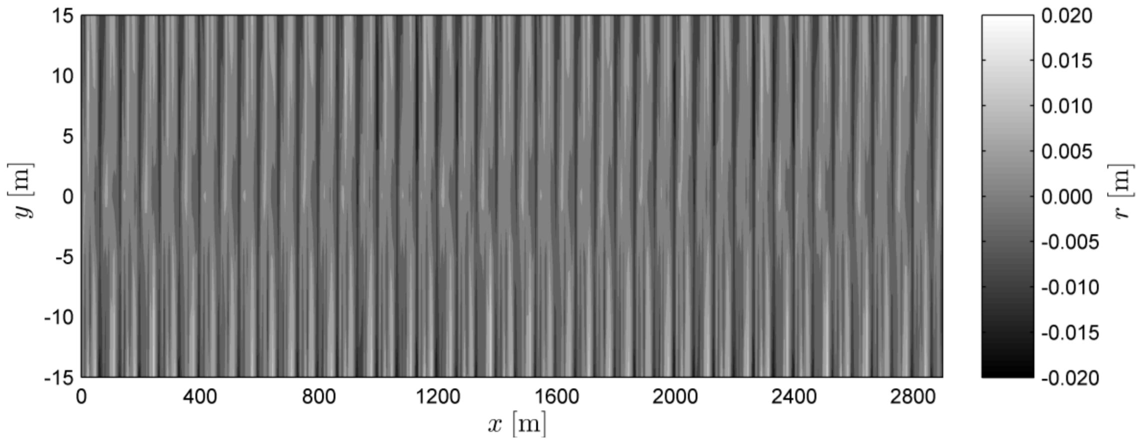

Figure 6. Generated correlated roughness profile.

3.2 Bridge response

The vertical dynamic response of the bridge for 15m/s wind with vehicle speed of 80km/h and 100km/h is shown on Figure 8. As expected, due to the very low frequency of the bridge, the interaction due to the roughness forces, with higher dominant frequencies, is quite small; however a vertical component due to the self-weight is obvious. If the vehicle is moving with V=100 km/h the bridge mid-point has a peak nearly at 70 s, while for V=80 km/h it is close to 90 s. The peak vertical displacement, however for the V=80 km/h vehicle is at 120 seconds, due to the wind forces. Comparing the RMS of the vertical response at mid span on Figure 8 for different models the variation of the peak displacement is up to 20%. As the wind velocity increases, the MBM model response decreases with respect to the LU and MQS due to the aerodynamic coupling. The MQS model response is higher than the LU due to the fluid memory. However, if the wind speed is closer to the flutter limit, this would in fact have reverse effect as with the lagging of the torsional motion, the effect aerodynamic coupling increases. Looking at the static wind coefficients on Figure 5, a preliminary indication is that the aerodynamic nonlinearity is negligible for the lift force. However, high nonlinearity is expected in the drag and the projection of the drag force to the vertical axis contributes to the lift, hence the response of the QS is higher than the LQS model. From the RMS over the span for U=20 m/s, one could guess the direction of traveling and an interesting point is made on the small deflection in the towers, as the structural system is not fixed on the towers location in the vertical direction. Generally, the models do not vary significantly in this range of wind speeds as the aerodynamic damping is low for low reduced velocities.

3.3 Vehicle response

The vehicle was simulated for each wind speed for vehicle speeds from 30 up to 130 km/h. Even if an accident occurred (negative contact force) the analysis was conducted until the last vehicle passes the bridge. On Figure 9 (left), the maximum contact force for the wheels with U=15m/s is depicted for the models. The variation is almost

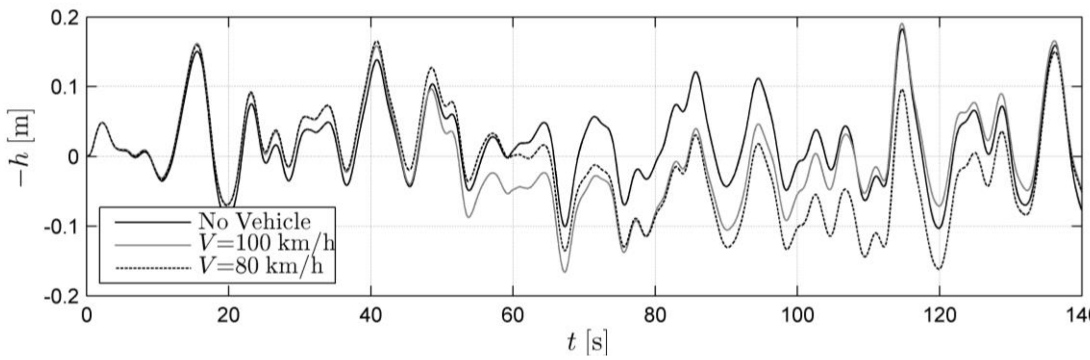

Figure 7. Bridge vertical dynamic response at mid-span for U=15m/s and different vehicle speeds.

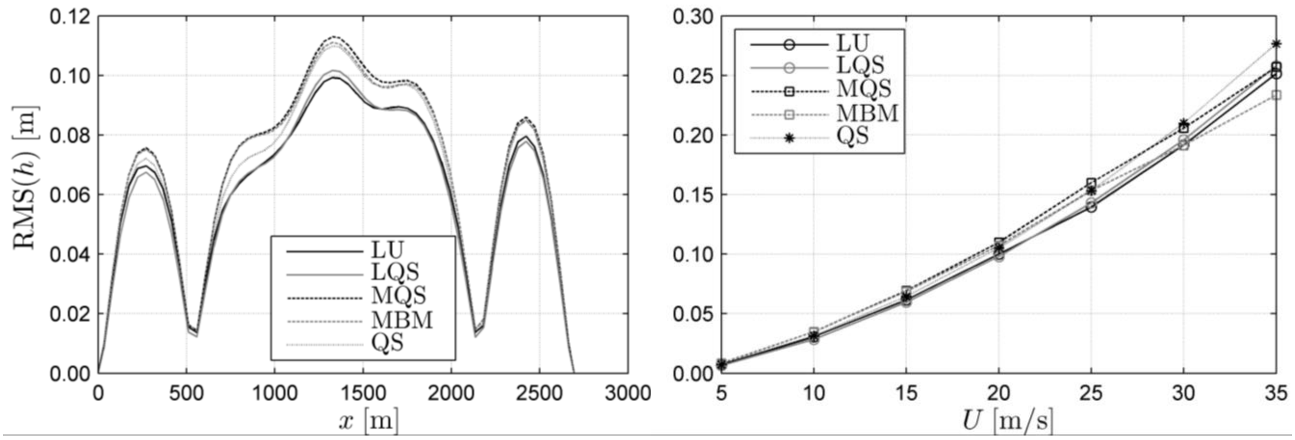

Figure 8. RMS of vertical disp. for different models: (left) span-wised for U=20m/s; (right) at mid-span.

negligible between the models, and the accident scenario is obtained when the line crosses at 0. On Figure 9 (right) the maximum contact force of a vehicle with 100 km/h is depicted for various aerodynamic models, resulting in negligible differences. The accident vehicle velocity for vehicle on the road and on the bridge is shown in Figure 10 (top-right). The critical speed decreases w.r.t. road accident speed as the as the wind-speed increases due to the larger wind-bridge interaction. The aerodynamic models resulted in similar results for the comfort criteria as well (Figure 10 (top-left)). This is expectable since in case of long-span bridges, the low structural frequencies result to low deck accelerations. Figure (bottom-left) compares the weighted, original and acceleration on perfect road for wind of 5 m/s. It is clear that the road roughness plays significant role in the comfort analysis. Xu and Guo [3] obtained similar results and relate the velocity-acceleration relation to the vehicle dynamic characteristics. Another possible explanation is that the speed changes the step-length of the vehicle; hence, the analyses for all vehicle speeds are conducted with a different roughness profile. This could be also seen if the weighted acceleration of the perfect road profile is observed, where there is an increasing trend. To alleviate this problem, a solution might be to study road profiles with the same roughness coefficient and a different random phase angle in order to obtain a statistical response. On Figure 10 (bottom right) – right the comfort is studied for different wind-velocities. It can be concluded that there is a general trend of an increasing acceleration with increasing wind speeds, and even the signals become less “nosy” indicating that the wind action is becoming dominant concerning the driver’s comfort. Furthermore, six levels of comfort are indicated according to ISO 2631 [3] ranging from comfortable L_1 to extremely uncomfortable level L_6. In conclusion, the vehicle response was independent of the aerodynamic model choice.

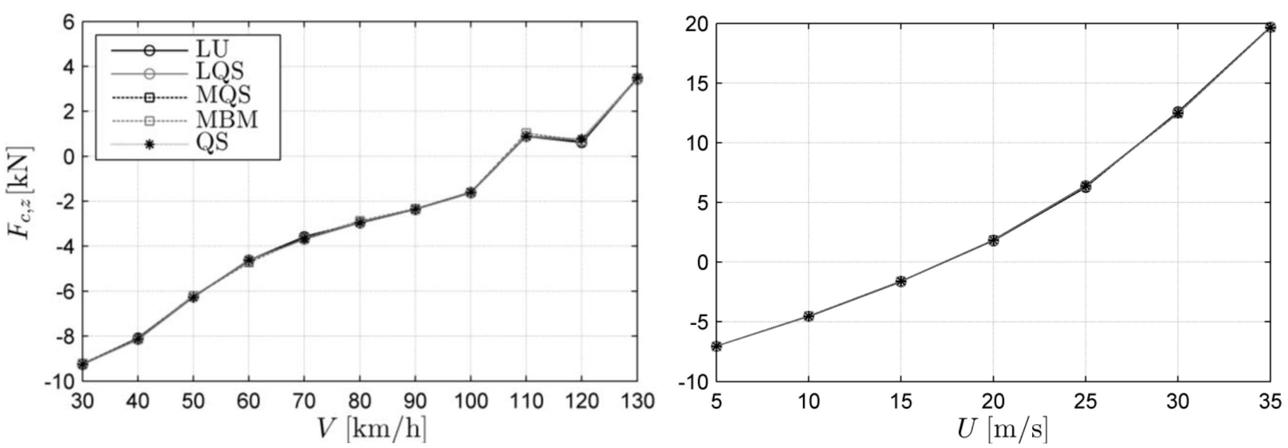

Figure 9 Contact force at the critical windward front wheel: (left) for U=15m/s; (right) for V=100 km/h.

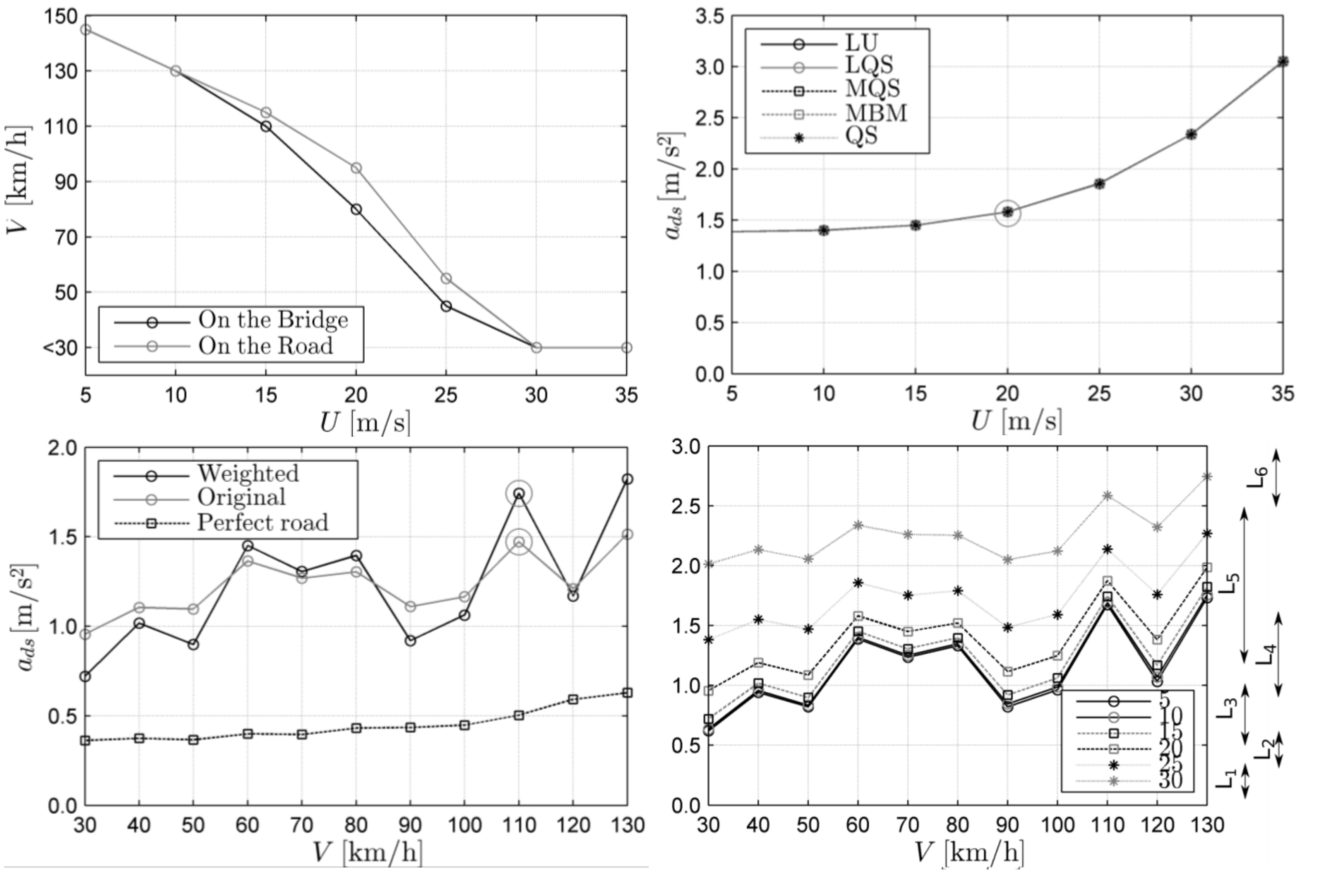

Figure 10. (top-left) Accident driving speed versus wind speed; (top right) Acceleration at driver's seat for V=100 km/h; (bottom-left) Weighted and original acceleration v.s vehicle speeds for U=15m/s; (bottom-right) Acceleration v.s. vehicle speed for various wind velocities. The gray circle marker indicates an accident.

4 Conclusion

The influence of various aerodynamic models for wind-bridge interaction was studied with respect to vehicle accident and comfort criteria. A suspension bridge is analysed for multiple wind velocities and vehicle velocities, for which the accident speed and comfort criteria are identified and were independent from the model choice. This is due to the fact that for the wind speeds in the range of interest, the implied assumptions are valid. Consequently, utilizing less complex model would lead to satisfactory results for the preliminary calculation. This is important as the complexity of the aerodynamic model increases the numerical and the parameter uncertainty increases as well. More complex models such as the modified quasi-steady model include identification of flutter derivatives, or even their by rational functions for the linear unsteady model. However, in the ultimate limit state, where these types of structures are prone to flutter, it is imperial to consider more complex models in order to replicate the occurring aerodynamic phenomena adequately.

5 References

[1] Han Y., Cai C.S., Zhang J., Chen S., and He X. Effects of aerodynamic parameters on the dynamic responses of road vehicles and bridges under cross wind. *Journal of Wind Engineering and Industrial Aerodynamics*. 2014; **134**: 78-95.

[2] Coleman S.A., and Baker, C.J. High Sided Road Vehicles in Cross Winds. Journal of Wind Engineering and Industrial Aerodynamics. 1990; **36**: 1383-1392.

[3] Xu Y.U., and Guo W.H. Effects of Bridge Motion and Crosswind on Ride Comfort of Road Vehicles. *Journal of Wind Engineering and Industrial Aerodynamics*. 2004; **92**: 641-662.

[4] Wu T., and Kareem A. Bridge aerodynamics and aeroelasticity: A comparison of modelling schemes. *Journal of Fluids and Structures*. 2013; **43**: 374-370.

[5] Larsen A.(ed.). *Aerodynamics of Large Bridges*. Proceedings of the First International Symposium on Aerodynamics of Large Bridges. Copenhagen; Balkema; 1992.

[6] Morgenthal G. *Aerodynamic Analysis of Structures using High-resolution Vortex Particle Methods*. Ph.D. Thesis, University of Cambridge, 2002.